# DETAILED SEISMIC TOMOGRAPHY IN RADIAL BOREHOLES

## 1. Background and Project Objectives and Method Selection

To obtain a better understanding of the properties of the disturbed zone and its dependence on the method of excavation, ANDRA (France), UK Nirex (UK) and SKB (Sweden) performed a joint study of excavation zone effects. The project, named ZEDEX (Zone of Excavation Disturbance EXperiment), is expected to contribute to the basis for selecting or optimising the construction method or combination of methods for a deep radioactive waste repository and subsequent sealing.

The fieldwork for the ZEDEX project was carried out at SKBs Hard Rock Laboratory (HRL) at Äspö, Sweden, in two parallel tunnels, one excavated by Drill & Blast and the other by Tunnel Boring Machine. The ZEDEX site at Äspö is located at 420 m depth below ground surface, in granite.

Seismic tomographic measurements were first performed during 1994 and 1995 and were primarily intended for the study of the far field, i.e. further than two meters from the wall of the excavation. The conclusion of these studies has been that the near field changes of the characteristics of the rockmass are predominant over the far field changes.

For the investigation of the near field, a detailed seismic tomography study was performed as part of the ZEDEX Extension Programme, in June 1996.

The objectives of the study have been the following:

1. To estimate the transverse extent, the seismic and elastic properties of the near field disturbed zone and of the transition zone from near field to far field,
2. To determine the relation between the seismic properties and the local stress,
3. To determine the seismic response of the rock features displaying outstanding rock mechanic and hydraulic properties, induced by the excavation of the drifts.

At the planning stage of the project it was anticipated that the excavation disturbance could be described in terms of effects in the near field, defined as the region within two metres from the excavation, and beyond that, the far-field, where the disturbance was expected to be independent of the excavation method.

Excavation disturbance effects can be measured, among others, by changes in seismic velocity. The seismic method selected for the investigation of the near field was a detailed tomography.

# 2. Project Planning

## *2.1 Scope*

The detailed seismic tomography study will performed in two fans of boreholes, one drilled in the TBM (Tunnel Boring Machine) drift and the other in the D&B (Drill & Blast) drift. Each fan consists of eight boreholes. The tentative plan is to drill the boreholes with a constant angular step of 45 .

The measurements will be performed from 0.075 m to 3.6 m depth. Due to the present construction of the measuring apparatus, the boreholes should be drilled to a depth of 4 m.

The depth increment of the measurements will be 0.075 m for the first 1.2 m of the boreholes and 0.15 m for the rest of the section, for both sources and receivers. The number of measurements for each section will be approximately 1000.

Due to expected difficulties with modelling wave amplitudes close to the tunnels, the tomographic analysis will concentrate on P- and S-wave velocities, including the modelling of possible anisotropy.

The results will be presented as color plots of P- and S-velocities and the dynamic elastic moduli Ed and Md. Additional plots will be provided for the angular variations of the velocities and anisotropy models.

## *2.2 Equipment*

The surveys will be carried out with the tool developed by Vibrometric Oy for high frequency (ultrasonic) borehole seismic studies. The main components of the equipment are the source and the multi-receiver probe. The probes have been designed for use in *56 mm* diameter boreholes in which they are clamped hydraulically.

The source module consists of a piezoelectric transducer, a power module providing the high voltage needed for driving the transducer, and two hydraulic pistons for clamping. The hydraulic pistons press the instrument against the borehole wall. The transducer is perpendicular to the borehole, and opposite to the hydraulic pistons. The source produces trains of pulses of pseudo-random lengths (one of five preset values) at pseudo-random time intervals. Various numbers of pulses of each type are added, in order to widen the frequency band of the source. The repetition rate is *10-20* stacks / second.

The receiver module contains eight piezoelectric transducers spaced at *0.15 m*. The transducers are aligned and perpendicular to the borehole axis. The hydraulic clamping system is similar to the one used for the source module.

The frequency band of the system is *5 - 60 kHz* and the investigation distance exceeds *20 m* in normally fractured rock.

An image of the receiver probe being introduced in a horizontal borehole is presented in Figure 1.


*Figure 1.*

*The ultrasonic borehole multi-transducer receiver probe being installed in a horizontal borehole*

## *2.3 Description of the Activity*

### *2.3.1 Mobilisation*

Mobilisation/demobilisation to site of the seismic probes, spare parts, computers and a senior geophysicist together with two assistants will be made from the contractors office in Helsinki, Finland. The senior geophysicist will be responsible for ensuring that the equipment arrives on site in time.

### *2.3.2 Calibration and function control*

The senior geophysicist will be responsible for ensuring that the equipment functions correctly and is calibrated and that the daily operation and calibration checklist is completed and signed. The equipment will be calibrated and operation checked each working day. Timing will be checked using a standard rod as connection between the source and receivers.

### *2.3.3 Measurement configuration and procedures*

Measurements will be made between eight borehole pairs in two fans of boreholes, one drilled in the TBM drift and the other in the D&B drift. The measurements will be performed as described in Section 2.1.

At each position of the source and receiver probes a sonic signal comprising 150 pulses (30 for each of five possible waveforms) will be transmitted from the source probe. Data received by the receiver probe (8 channels) will be automatically processed and recorded by computer. The data will be checked visually on the terminal and, if it appears satisfactory, the position of one of the probes will be changed and the measurement repeated. The complete measuring sequence: transmit; receive; process; and move is expected to take about 2 minutes on average.

The data will be backed-up on suitable magnetic media and one complete copy will be delivered to SKB's data manager for safekeeping.

### *2.3.5 Demobilisation*

The senior geophysicist will contact the Äspö database manager to confirm that all data has been correctly supplied. Thereafter demobilisation will be the reverse of mobilisation.
It is expected that the field work will be completed within 2 weeks from the mobilisation.

### *2.3.6 Data processing and interpretation procedures*

Data processing is the responsibility of Vibrometric Oy and will take place on return to the office. The processing will be performed for data from the fan in the *D&B* and *TBM* drifts. Due to expected difficulties with modelling wave amplitudes close to the tunnels, the tomographic analysis will concentrate on P- and S-wave velocities, including the modelling of possible anisotropy.

The results will be presented as color plots of P- and S-velocities and the dynamic elastic moduli Ed and Md. Additional plots will be provided for the angular variations of the velocities and anisotropy models.

The results will be reported in a Technical Note according to specified format.

It is expected that this activity will be completed within 4 weeks of leaving site.

## 3. Performance of the Survey - Field Work

The field work was carried out in two fans of radial boreholes: the *D&B* Round 7 and the *TBM* Round 2.

At the start and the end of each day the timing accuracy of the equipment was checked by recording signals propagating through a calibrated aluminium rod placed in turn between the source and each of the receiver elements. The recording was done on one channel, at the maximum time resolution of *1 ms*. The response of the analogue system was found to be within the 1 *ms* digital accuracy limit.

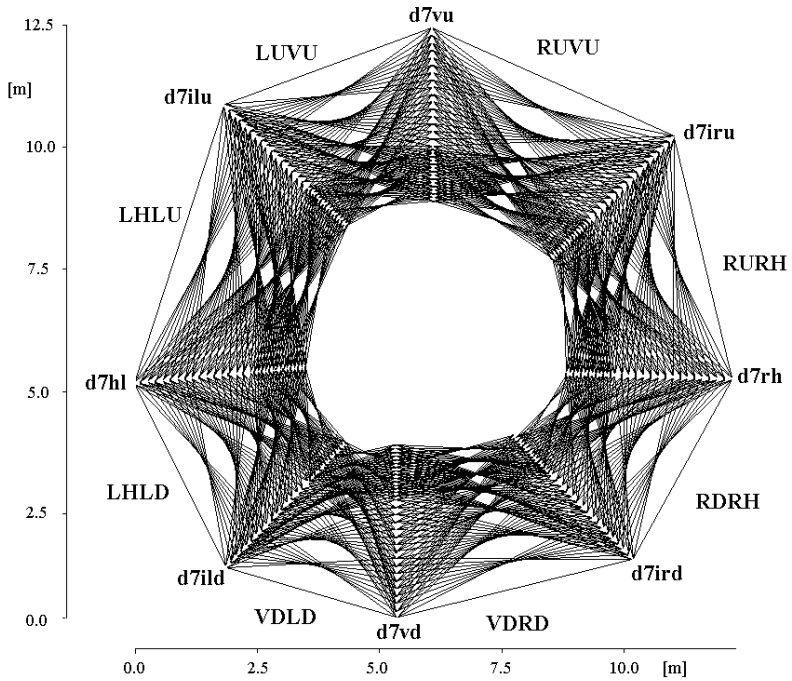


*Figure 2. Ray diagram of the eight crosshole sections measured around the D&B tunnel. Every section is identified by the corresponding pair of boreholes. The first borehole in the name of the section is the source borehole. Similar coverage was achieved around the TBM tunnel (borehole names start with t2, instead of d7, in this case).*

The measurements were performed as eight crosshole layouts between pairs of adjacent boreholes, for both the *D&B* and the *TBM* drifts, as exemplified in Figure 2. The depth increment between subsequent source and receiver positions was *0.075 m* for the top *1.25 m* and *0.15 m* for the rest of the section, to *3.6 m* depth. This produced a more densely covered zone close to the tunnel. The number of measurements for each section was *1024*, i.e. *32* sources and *32* receivers. Figure 2 displays one eighth of the actual number of measurements.

For all measurements, both the source and receiver probes were placed with the transducers at $45^o$ degrees from the plane of the boreholes pointing towards the other borehole. Figure 3 illustrates this arrangement.

At each position of the source and receiver probes, a sonic signal comprising *150* pulses (*30* for each of five possible waveforms) was transmitted from the source probe. Data received by the receiver probe (*8* channels) were automatically processed and recorded by computer. The data were checked visually on the terminal and if it appeared satisfactory the position of the source probe was changed and the measurement repeated until the whole-intended length was covered with the source. Then the receiver probe was moved to the next position. The complete measuring sequence: transmit; receive; process; and move lasted about *2* minutes on average.

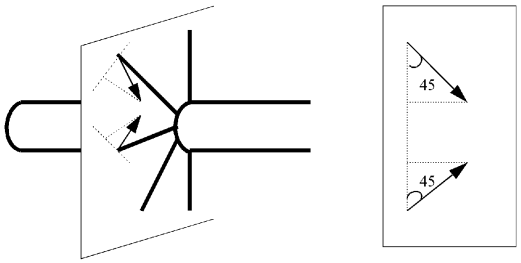


*Figure 3. Orientation of the transmitter and receiver probes with respect to the tunnel and the plane of the boreholes.*

# 4. Data Processing and Interpretation

## *4.1 Arrival Time Picking, Time Corrections*

A two-step procedure was used for picking the P-wave arrival times.
Rough estimates were obtained by applying cross-correlation and neural networks based algorithms to data filtered in the band *5 - 32 kHz*. The shape of the first onsets was found to be extremely stable in this band, as one can notice in Figure 4. Due to the stability of the signal shape, covariance analysis within a rectangular window including *5* neighbouring sources by *5* neighbouring receivers yields as good a results as the neural networks approach, at a fraction of the processing time. The precision of this preliminary pick was of *+/- 6 ms* for appr. *96 %* of the data. The remaining *4%* of the data were eliminated.

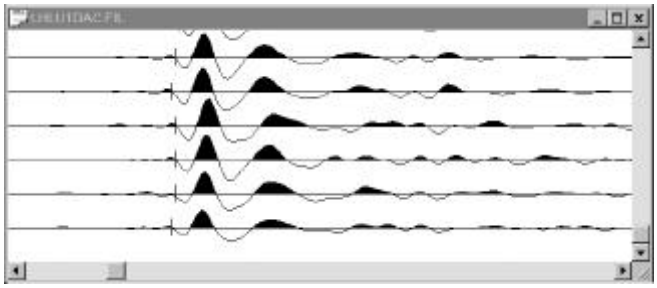

*Figure 4. Part of the D&B LH-LU section bandpass filtered from 5 to 32 kHz.*

The non-filtered data were re-sampled fourfold, bringing the sampling rate to *1 ms*. The arrival times picked from the filtered data were than brought to a precision of *+/-1 ms* by cross-correlating the signals of adjacent ray paths with a time lag of. *+/-5 ms*. A set of traces is presented in Figure 5, illustrating the time picking procedure.

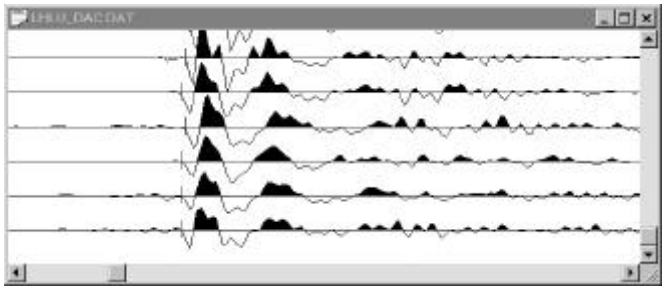

*Figure 5. The data subset from Figure 4, without filtering, resampled fourfold.*

Due to the very precise time picking procedure, a periodic drift of the travel times could be observed, with respect to the receiver positions. The drift is due to the *1 ms* delay between the channels connected to the same A/D converter. As two A/D conversion boards with four channels each were used in parallel, the period of the drift is *4 ms*. An example of such systematic errors is given in Figure 6a, which shows time residuals corresponding to a constant velocity of *5950 m/s* as a function of the receiver positions. Figure 6b displays the same distribution with the times corrected for A/D conversion lags. We should stress here that the phenomenon depicted in Figure 6 confirms the precision of the time picks estimated to *+/-1 ms*.

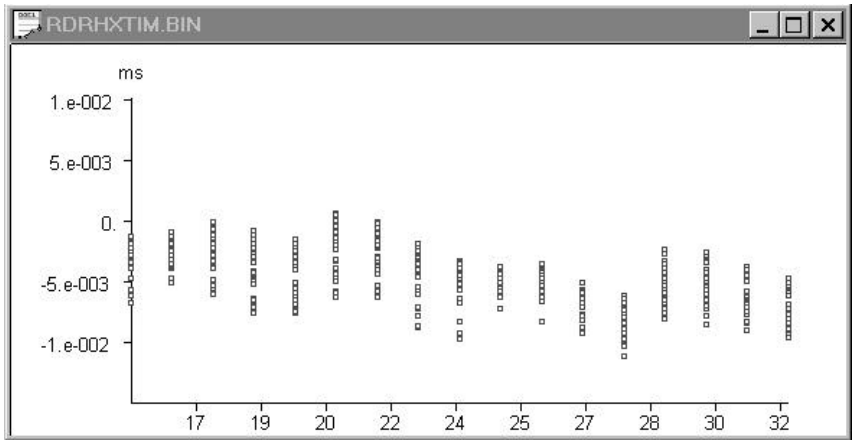


*Figure 6 a) Original distribution - reduced time vs. detector number*

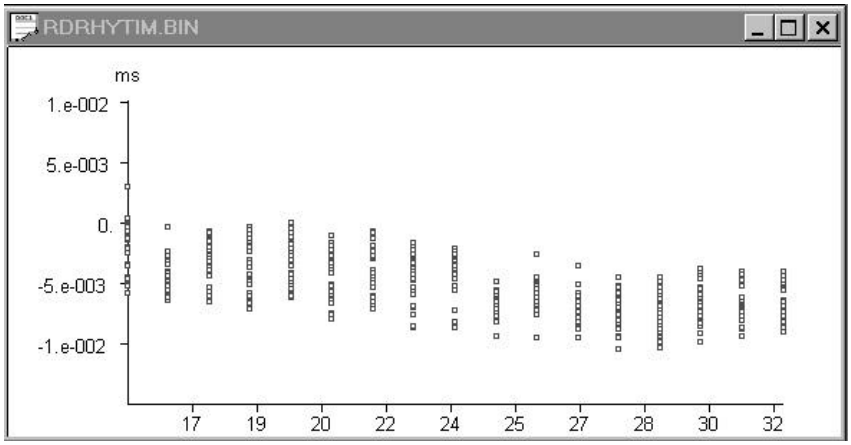


*Figure 6 b) Corrected distribution*

*Figure 6. Time correction to compensate for A/D conversion, 1ms lag.*

Figure 7 displays two trace gathers recorded from the *TBM* drift, by a receiver placed at *1.35 m* depth in borehole *t2VD* . The sources were placed in borehole *t2ILD* and *t2IRD*, respectively.

The gathers are presented in reduced velocity mode, for a velocity of *6050 m/s*, i.e. signals travelling with an average velocity of *6050 m/s* line up vertically. Deviations of the first arrivals to the left and to the right signify higher and lower velocities, respectively.

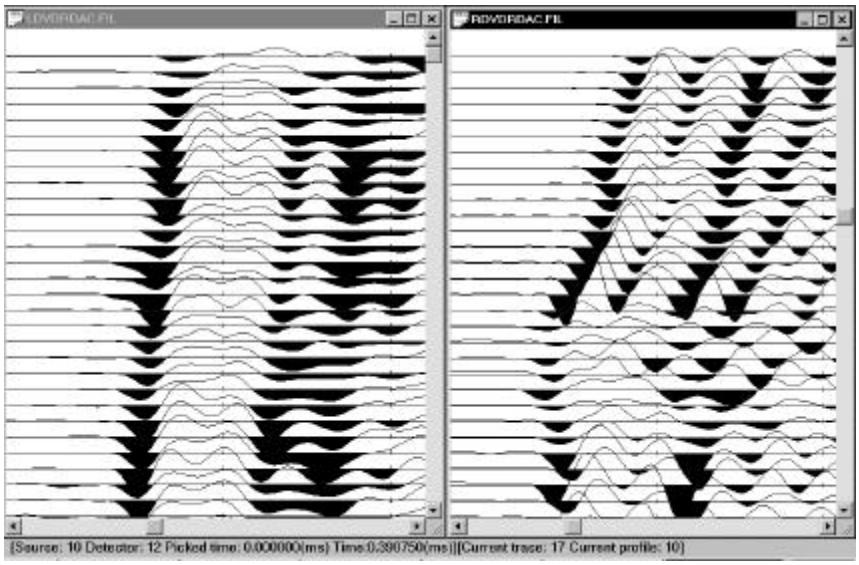


*Figure 7. Trace gathers in sections LDVD and RDVD, TBM tunnel.*

The profile on the left of Figure 7, belonging to the section *LDVD*, *TBM* drift, displays a smooth velocity distribution, slowly increasing with the depth. The velocity is *6100 m/s* on the first trace and *6160 m/s* on the last. The profile on the right belongs to the section *RDVD* and its appearance is very different from its neighbour. The velocity of the first five traces is comparable in the two profiles. For deeper sources, the velocity increases in the profile *RDVD* and reaches a maximum of *6400 m/s* for the detector placed at a depth of *1.35 m* in *t2VD*.

The behaviour described above is not limited to the two sections bordering the borehole *t2VD*. An even stronger asymmetry can be seen between profiles *LDLH* and *RDHR*. Figure 8 presents two trace gathers recorded from sources placed at *0.75 m* depth in boreholes *t2ILD* and *t2IRD*. Here too the profile on the right has a strange appearance, displaying a maximum velocity of *6600 m/s*. This is a very high velocity indeed and the presence at Äspö of geological formations of such high velocity has not been reported to date. The question which arises is whether a systematic measuring error could produce such artifacts.

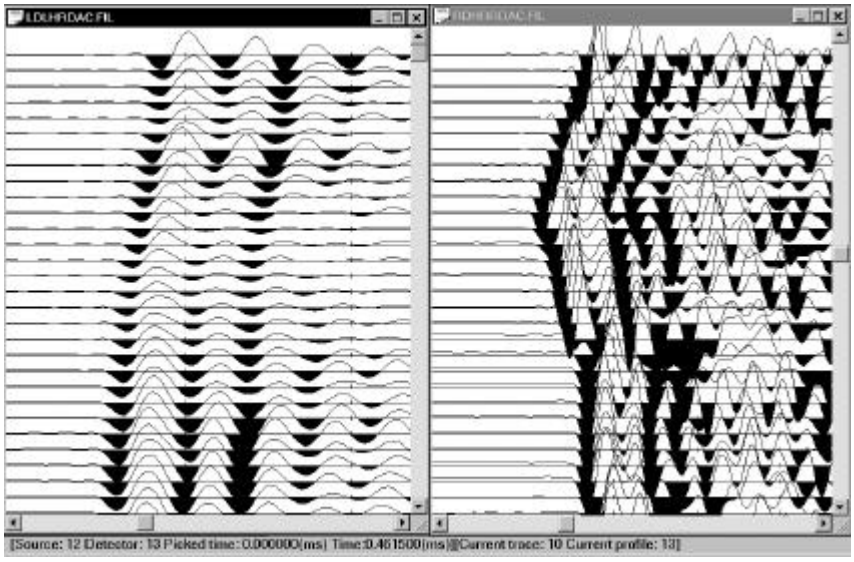

*Figure 8.*
*Trace gathers in sections LDHL and RDHR, TBM tunnel.*

An erroneous velocity can be attributed to timing due to one of the following reasons:
1. false triggering,
2. inaccurate digitising clock,
3. wrong time picks.

False triggering is ruled out because it would show as a time lag of comparable magnitude on each of the eight channels recorded simultaneously.

Unstable digitisation would produce random delays. On the contrary, the A/D conversion lag of 1 μs appears consistently, as seen in Figure 6. Such minute trends would be impossible to see if superposed on random errors an order of magnitude higher.

Regarding time picking, the deviations back and forth from the vertical of the first arrivals in Figures 7 and 8 are self evident, and no "correct" time picking would convince them to become vertical.
We must conclude that, as far as the events presented in Figures 7 and 8 are first P-wave onsets, the abnormally high velocities can not be explained by timing errors.

## *4.2 Borehole Coordinates, Position Corrections*

The position in space of each borehole has been given only as two coordinate triplets, one for the beginning, the other for the end of the borehole. Therefore, it is reasonable to assume that, if they are accurate enough, these coordinates refer to the axis of the borehole. On the other hand, the seismic transmitter and receiver probes were pressed against the borehole wall and positioned as shown in Figure 9. Therefore, the distance between a transmitter and a receiver placed at the same depth in two adjacent holes is roughly 4 *cm* shorter than computed from the borehole coordinates. For a distance of two meters, the corresponding error in velocity is appr. *120 m/s*. For comparison, the velocity variation corresponding to the *1 ms* estimated time error is *20 m/s*. A velocity error of the same magnitude would be produced by a positioning error of *7 mm*. It would be indeed very difficult to maintain such a strict positioning accuracy for all the holes from top to end. However, the positioning corrections described above induced a detectable improvement of the consistency of the data.

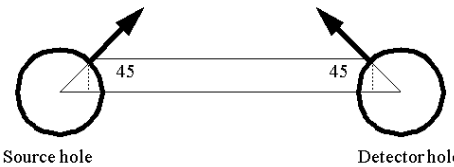


*Figure 9. The true source - receiver distance is AB. The borehole coordinates give the segment OO.*

Positioning errors may appear also along the holes. This is the most probable cause of a significant anisotropy noticed only in the two sections containing borehole *R7ILD,* from the *D&B* drift. The anisotropic behaviour vanished after shifting the all stations in this hole *7.5 cm* outwards. The error has been produced by the lack of an clearly marked reference of the borehole top. This problem did not appear for the boreholes which had flat collars.

Positioning errors which may appear along the holes can also be due to the borehole coordinates or to wrong readings of the borehole depth of the seismic transducers. To test the latter hypothesis, for the measurements made in the TBM drift, we have attempted to minimise the tomographic residuals by shifting the positions of the measuring probes along the borehole axes. A discussion of the results will follow, in Section 5.2. We will note here only that we did not find a combination of systematic shifts along the boreholes, leading to the cancellation of the velocity anomaly crossing the lower right part of the Round *2* borehole fan. The following two hypotheses could not be tested due to lack of supporting information:

a) Some boreholes are actually shifted along the tunnel with respect to their reported positions and/or deviate from their reported directions. The possible causes include borehole bending. The highest deviation would occur with borehole *t2IRD*.
b) There is a high velocity elongated body in the immediate vicinity of the TBM tunnel which should be found in borehole *t2IRD* at a depth of *0.65-0.85 m*

### *4.3 Tomography*

By tomographic inversion, the information obtained from field measurements is transformed to a model of the structure of the rock. Several methods can be used, depending on the complexity of the structure and the resolution requirements. A bent-ray SIRT algorithm, with smoothing of the solution after every iteration, was used for the tomographic inversions. In order to decide on the method, trials have been done with straight ray routines and faster converging inversion algorithms. However, the use of bent ray did not produce any noticeable change further than half meter of the tunnel.

## 5. Results

### *5.1 Measurements in the D&B drift*

One-dimensional inversions were run for both P- and S-waves by allowing the velocity to vary only along the mid-line of the two boreholes, in each section. This resulted in distributions of the velocity vs. the distance from the tunnel. The Young and Shear modulus were also computed, assuming a density of *2600 kg* $m^{3.}$

One of the eight groups of diagrams is shown in Figure 10. Adjacent sections have many common characteristics, changing gradually to the farther sections. A slight difference can be observed between the sections above the horizontal mid-plane of the tunnel and the ones below.

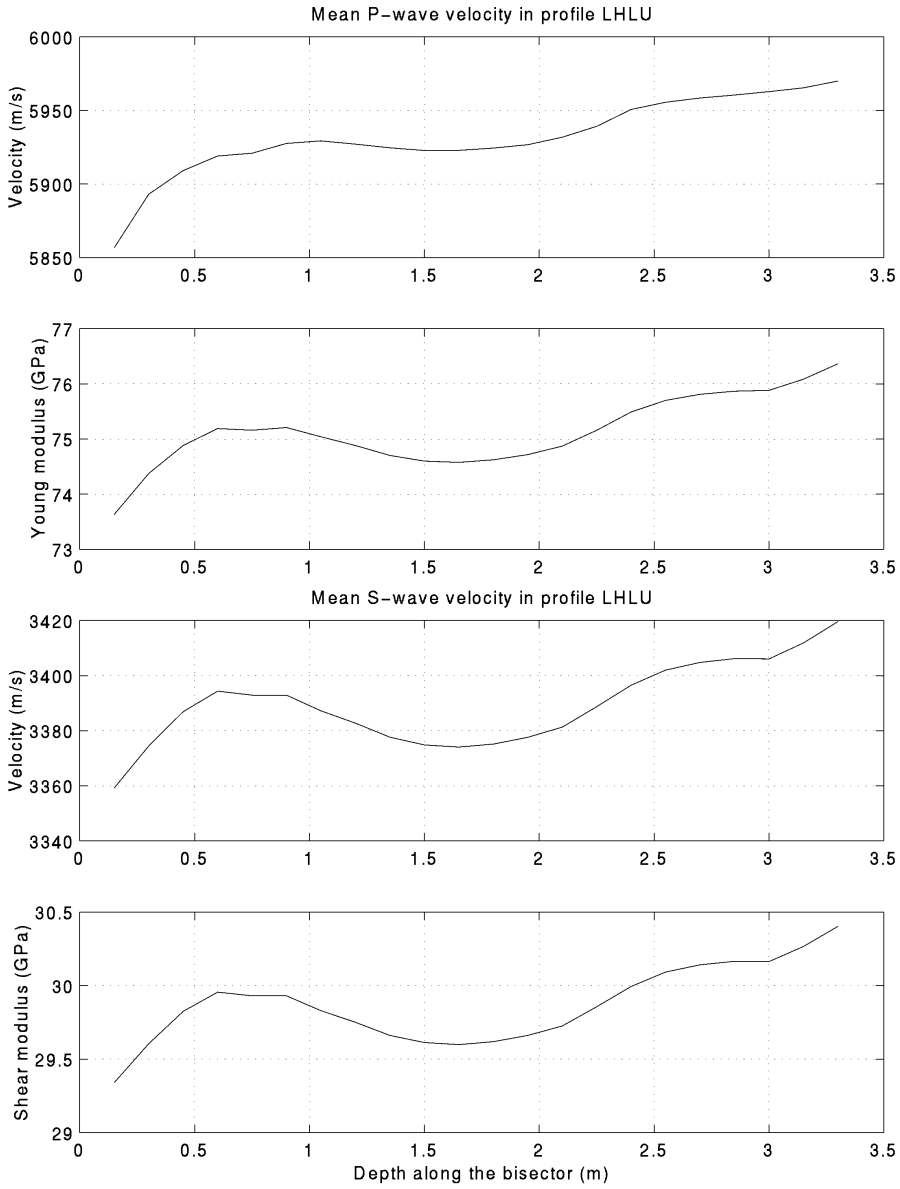


*Figure 10. Section LHLU, along the borehole-mid-line, D&B round 7.*
a) P-wave velocity, *b)* Young modulus, *c) S-wave velocity, d) Shear modulus.*

Generally, the P-wave velocity climbs over *5900 m/s* in the first *20 cm* to 5*0 cm* and stays between *5900 m/s* and *6000 m/s*. A gently sloping part of the diagrams follows to *1.5 m* to *2.5 m*. One may also note that the S-wave diagrams have a certain resemblance to the ones for P-waves. For both types of waves, the velocity variations in the deeper parts of the sections are of only of a few tens of *m/s*.

Each of the eight diagrams was obtained from appr. *1000* time picks for P -waves and a roughly equal number for S-waves. One could expect a very high stability of the result, due to the strongly over-determined inversion. However, the averaging can not cancel the velocity bias resulting from minute positioning errors. It is estimated that the measuring positions in seven of the eight boreholes are accurate within a *10 mm* interval, which corresponds to appr. a *30 m/s* P-wave velocity bias. In deed, there are no larger velocity variations in the deeper

rock, with the exception of the section LU-VU, for which the velocity variation along the mid-line is about 60 m/s.

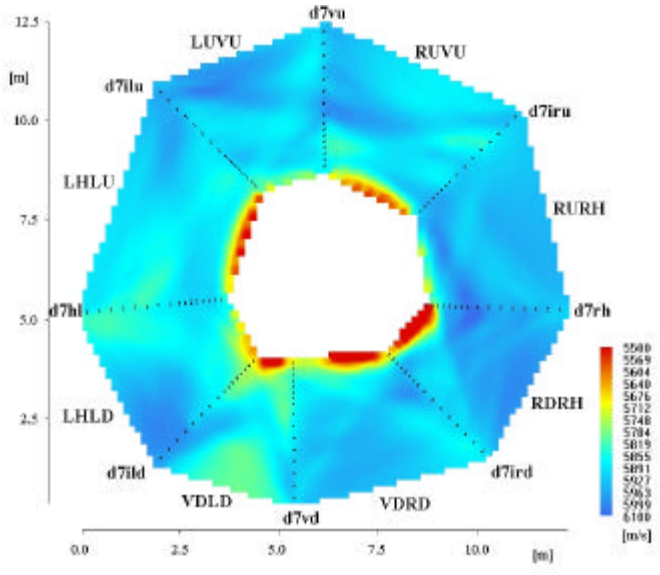


*Figure 11.*
*P-wave velocity of the eight crosshole sections of D&B round 7. One notes the ring of lower velocity around the tunnel and the constant velocity elsewhere.*
*The mean velocity is 5937 m/s and the residual mean square error after inversion was 1.53 ms. The inversion was done on 7996 travel times with 0.15 m X 0.15 m block size.*

Two-dimensional inversions were run both for P- and S-waves. A tomographic section for P-waves can be seen in Figure 11. No corrections were used, except for the ones described in Sections 4.1 and 4.2. Unlike the one-dimensional inversions, the two-dimensional tomographic inversion from Figure 11 was computed for all the eight sections at a time. The lighter shade at the bottom of the section LD-VD would correspond to an anisotropy of *1.5 %* but this is believed to be still due to minute errors of positioning, rather than to genuine anisotropy. The variations of the velocity with the path direction are less than *1 %* in the other sections.

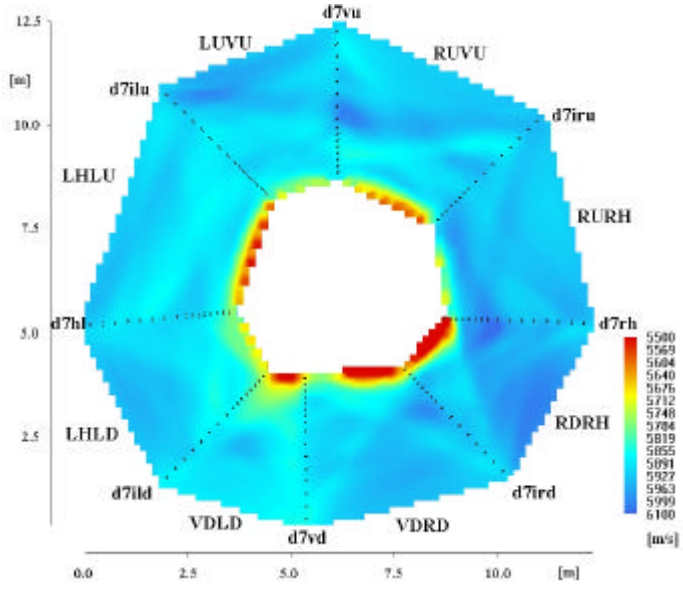


*Figure 12.*
*P-wave velocity of the eight crosshole sections of D&B round 7 after correcting for anisotropic effects. The anisotropy was 1.5% in section VDLD and less than 1% in the other sections. .*
*The mean velocity is 5938 m/s and the residual mean square error after inversion was 1.41 ms. The inversion was done on 7996 travel times with 0.15 m X 0.15 m block size.*

After correcting for systematic angular variations, a new tomographic inversion of the whole *8*-section data set produced the distribution from Figure 12, which is remarkably flat, with the exception of the immediate vicinity of the tunnel.

The tomographic inversions for S-waves were hindered by the occurrence in certain parts of the data of a double S-wave pulse, with a time lag of less than *10 ms*, as seen in Figure 13.

The de-synchronization of the records is ruled out as a possible explanation, as the P-waves picked from the same traces fall perfectly in line. It should be noticed also that the two pulses co-exist on some traces and one or another takes the lead in each direction. Shear wave splitting seems to be a reasonable explanation, which does not contradict the negative result regarding the P-wave anisotropy. Indeed, *10 ms* lag for S-waves would translate in a velocity variation of 1% or less. This variation would remain probably under the acceptable error limit set by the positioning precision. The repeated occurrence of such double S-arrivals through out the data sets may point to a measurable way to estimate anisotropy. The method would be more reliable than the direct computation of velocities because it is less dependent on the difficult positioning problem.

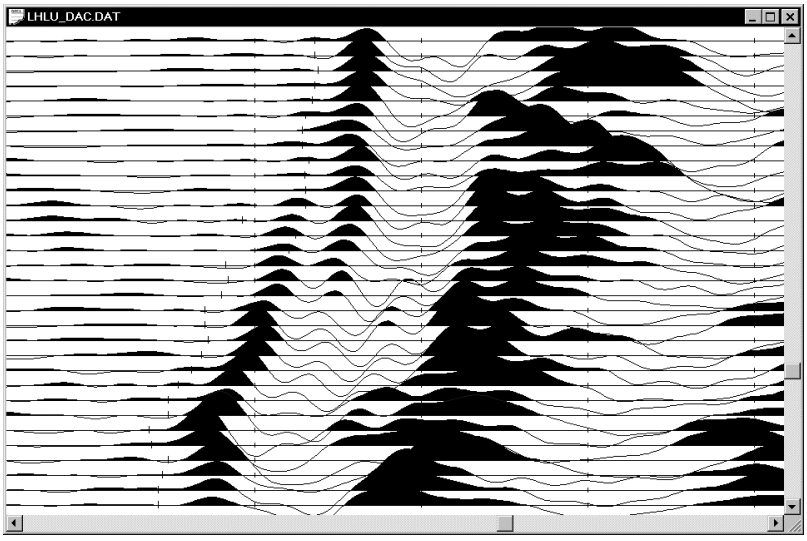


*Figure 13.*
*Part of the section LHLU, of D&B round 7, plotted with reduced velocity v= 3450 m/s. With this presentation, shear wave arrivals should be roughly vertical. One notes the double S-wave arrival, probably due to splitting. If due to anisotropy, the velocity ratio between SH and SV waves corresponding to such splitting is estimated to 1% or less.*

## *5.2 Measurements in the TBM drift*

Two-dimensional inversions were run for P-waves for all eight sections.
Due to the anomalous behaviour of the lower right corner of the borehole fan, the inversion was repeated with various corrections applied. The inversion was computed for all the sections at a time.

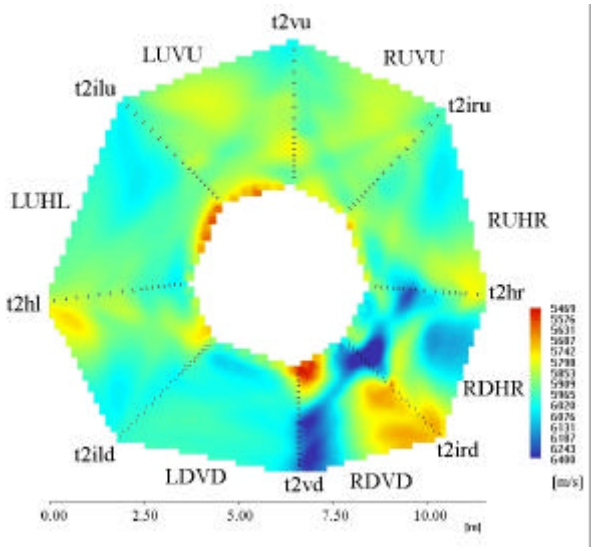


**The tomographic section in Figure 14 was obtained with no corrections,** except for the ones described in Sections 4.1 and 4.2. It is apparent that sections *RDHR* and *RDVD* have a pathologic appearance.

*Figure 14. P-wave velocity of the eight crosshole sections of TBM round 2.*

*The mean velocity is 5987 m/s and the residual mean square error after inversion was 1.96 ms. The inversion was done on 7979 travel times with 0.15 m X 0.15 m block size.*

**The tomographic section Figure 15 shows the velocity distribution with position shifts along the borehole axes.** The smallest errors were obtained for the following shifts:

- *t2HR*: *5 cm* out,
- *t2IRD*: *8 cm* out,
- *t2VD*: *9 cm* in.

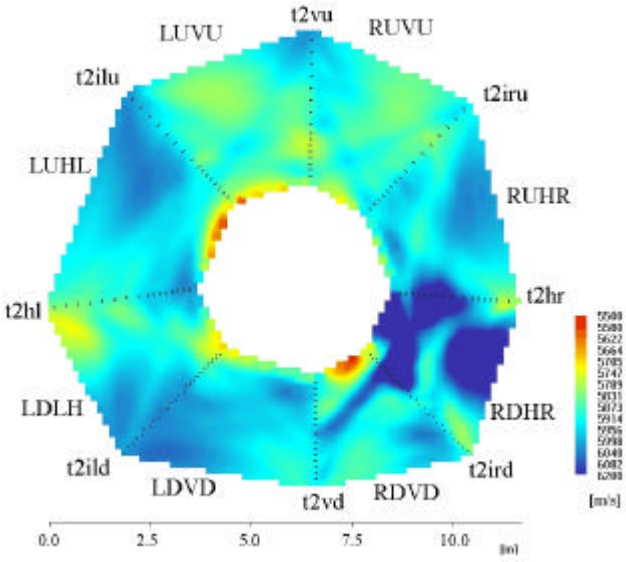


*Figure 15. P-wave velocity of the eight crosshole sections of TBM round 2.*

*The mean velocity is 5994 m/s and the residual mean square error after inversion was 2 ms. The inversion was done on 7979 travel times with 0.15 m* X *0.15 m block size.*

The hypothesis tested was that the borehole depths of the instruments in boreholes *t2HR*, *t2IRD* and *t2VD* could have been wrongly marked in the field logs, although there is no supporting evidence for such an error. Sudden time shifts in the recorded data would appear, indicating the moment when such an error had occurred. This not being the case, all positions in the same hole were shifted with the same amount.

The high velocity zone is still there, but it came down to more physically acceptable values.

**In Figure 16, anisotropic corrections were computed separately for each section**. Although this approach is not entirely justified, it has been used here in the attempt to correct for all factors producing anisotropic effects, including genuine anisotropy and unknown positioning errors.

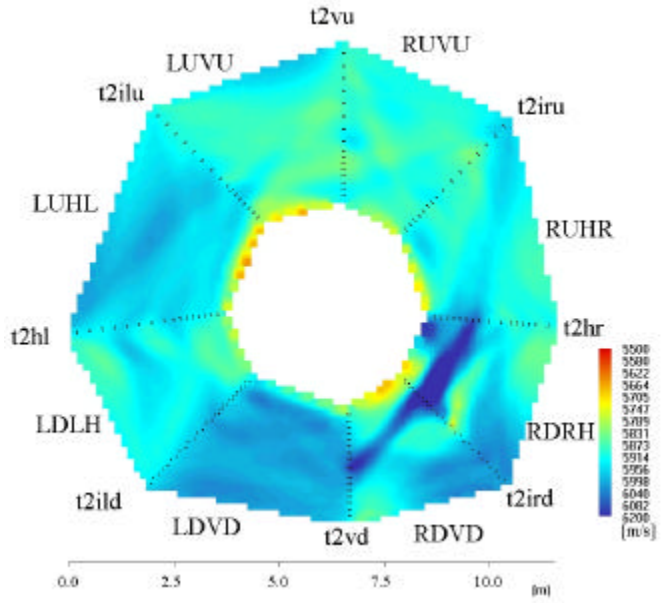


*Figure 16. P-wave velocity of the eight crosshole sections of TBM round 2.*

*The mean velocity is 5984 m/s and the residual mean square error after inversion was 1.53 ms. The inversion was done on 7979 travel times with 0.15 m* X *0.15 m block size.*

The velocity distribution became remarkably flat, with the exception of the high velocity anomaly crossing sections *RDHR* and *RDVD*. The high velocity feature becomes more consistent after the anisotropic correction, it continues through both sections and is probably real.

The low velocity zone in the vicinity of the tunnel is very thin and an attentive look would reveal that it actually falls closer to the tunnel axis than any of the sources and receivers. Therefore, it is probably a reconstruction artifact, due to the poor ray coverage at the edges of the tomogram.

**In Figure 17, we have applied the same anisotropic correction scheme to the original data set** (Figure 14) as to the data set with shifted positions in the boreholes (Figure 15).

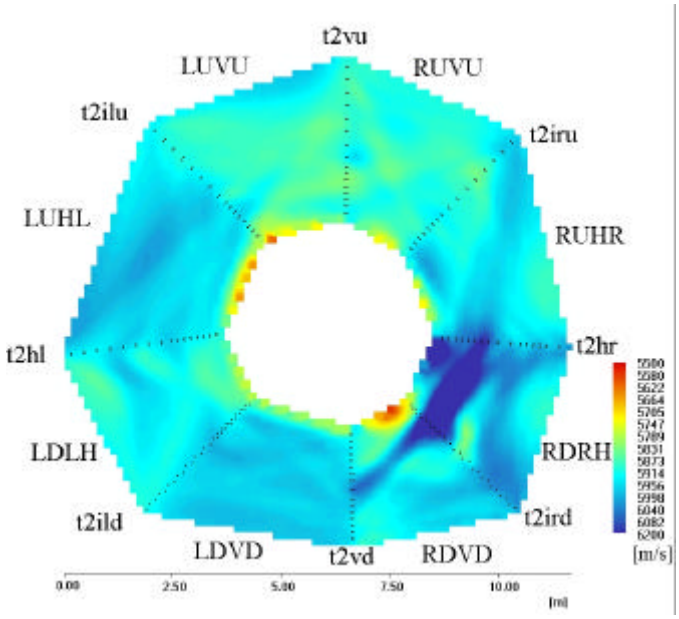


*Figure 17. P-wave velocity of the eight crosshole sections of TBM round 2.*

*The mean velocity is 5992 m/s and the residual mean square error after inversion was 1.54 ms. The inversion was done on 7979 travel times with 0.15 m X 0.15 m block size.*

This was done to prove somehow that the application of anisotropy corrections separately for each section manages indeed to cancel positioning errors. The result is practically identical to Figure 16.

**The situation can be summarised as follows**:

a) From the eight crosshole sections forming the tomographic image, six produce normal velocity distributions.

b) The two remaining sections, *RDHR* and *RDVD*, display an abnormal anisotropy and a high velocity feature.

c) Shifting the borholes along their respective axes did not eliminate the anisotropic behaviour but largely reduced it. Therefore, the anisotropy is believed to be an artifact produced by positioning errors.

d) The correction based on least square fitting of a three-parameter anisotropic model compensates for both real anisotropy and wrong positioning. In the case of erroneous positioning, the relation between the parameters of the elastic model looses its physical meaning, but the method will still be effective in suppressing the systematic dependence of the velocity with the direction of propagation.

e) If the method is indeed effective for correcting errors of positioning, additional adjusting of the positions before applying the correction should not affect the result. This is proven by the similarity of Figures 16 and 17.

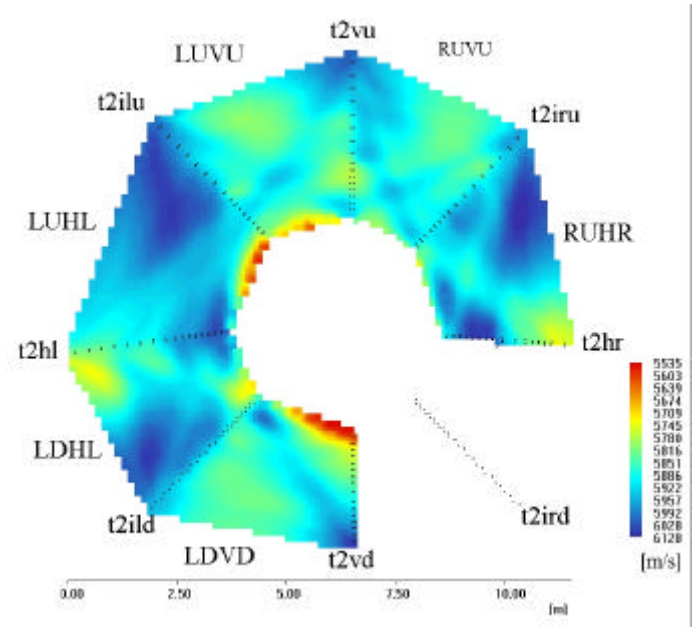


The six “normal sections” produce the tomogram from Figure 18. The velocity .vs. angle distribution is presented in Figure 19. In this case, the anisotropy is probably real. Its direction is exactly vertical and its magnitude is 2 %.

*Figure 18. P-wave velocity of six crosshole sections of TBM round 2.(Sections RDRH and RDVD were ignored.)*
*The mean velocity is 5995 m/s and the residual mean square error after inversion was 1.51 ms. The inversion was done on 5995 travel times with 0.15 m X 0.15 m block size.*

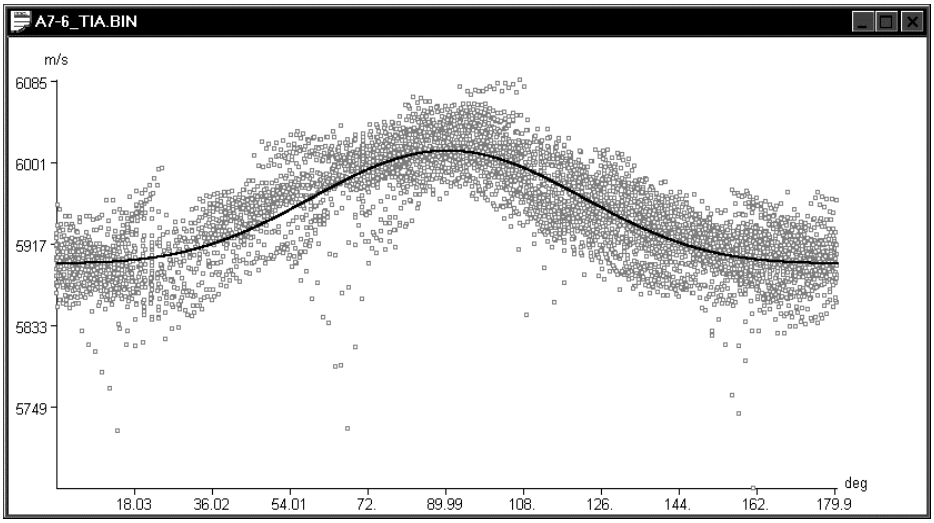


*Figure 19. Velocity vs. Angle distribution for six sections. The number of data points is appr. 6000. The curve represents the least squares fit of an anisotropic model with three parameters. The best fit values are: maximum velocity (model) 6050 m/s, direction of maximum velocity - vertical, elliptical variation (period p) 2%, secondary variation (period p/2) 0.45 %.*

After anisotropic corrections, the velocity distribution is plotted in Figure 20.

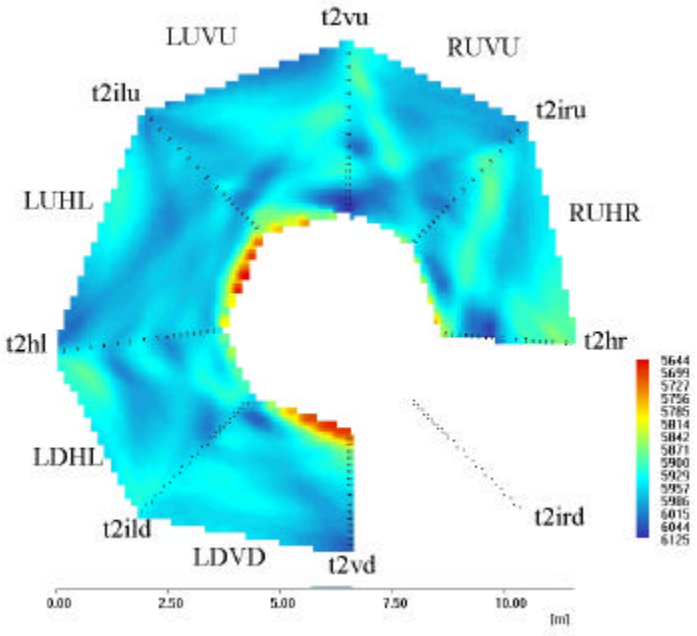


*Figure 20. P-wave velocity of six crosshole sections of TBM round 2, after applying corrections. (Sections RDHR and RDVD were ignored.)*
*The mean velocity is 5993 m/s and the residual mean square error after inversion was 1.21 ms. The inversion was done on 5995 travel times with 0.15 m X 0.15 m block size.*

One-dimensional inversions were run for both P- and S-waves by allowing the velocity to vary only along the mid-line of the two boreholes, in six of the eight sections. This resulted in distributions of the velocity vs. the distance from the tunnel. The Young and Shear modulus were also computed, assuming a density of *2600 kg* $m^{3.}$

One of the six groups of diagrams is shown in Figure 21.

The P-wave velocity is over *5900 m/s* with the exception of the first *10 cm* in the section *LDVD*. One may conclude that there is no detectable damage around the *TBM* tunnel.

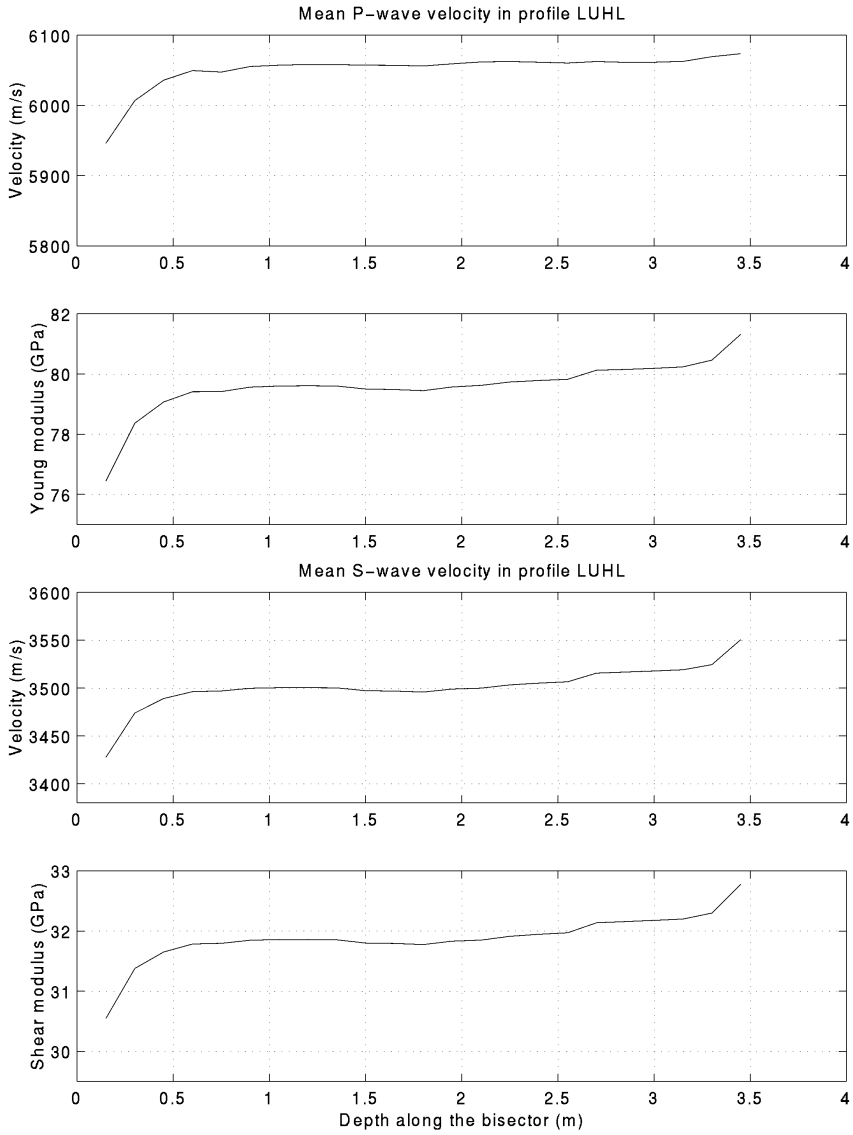


*Figure 21. Section LUHL, along the borehole-mid-line, TBM round 2.*

*a) P-wave velocity*
*b) Young modulus*
*c) S-wave velocity*
*d) Shear modulus*

## *5.3 Conclusions*

Changes in the seismic properties associated to the excavation damage were noticed within *0,5 m* from the tunnel. A zone of smaller contrast extends to *1.5* to *2.5 m* and has a different shape for the upper and the lower part of the fan of boreholes.

Anisotropy of the P-wave velocity has not been noticed. The S-wave analysis has not been as detailed as for P-waves.

One has to stress again the need of very high precision in both time picking and positioning. Accurate time picking can be easily controlled, if it is given attention already when specifying the data acquisition apparatus and calibrations and checks are performed regularly.

The experimental apparatus used for the ZEDEX seismic tomography was found enough precise, in terms of its analogue components, i.e. source timing, receiver time lags, frequency content, bandwidth, output power and sensitivity of the receivers. The analogue to digital conversion at a rate of *4 ms* was less performing and, in fact, the processing could not have been done properly without using state-of-the-art resampling routines, to bring the sampling rate to *1 ms*. For future tests, the experience accumulated at ZEDEX could be used to specify an even better tool. Compared with the existing version the new acquisition apparatus will have the following added features:

- Simultaneous recording of two components, for each of the *8* receiver modules (*16* channels instead of *8*);
- A choice of transducer types, to adjust the frequency band and the directivity function of the receivers;
- Each receiver module can be assembled either in an axial-transversal (Z-T) or in radial-transversal (R-T) configuration.

The Z-T configuration will be used e.g. with the single hole and inverse VSP layouts for recording both P- and S-waves travelling more or less along the hole.

The R-T configuration is intended for producing simultaneously P- and S-wave transmission crosshole profiles.

The source module will contain two sources, arranged either as a R-T or a Z-T pair. Together with the two-component receivers, four-component profiles can be recorded. This will provide full angular coverage for both P- and S-wave reflection studies. In transmission mode, the *4*-component records will make the tomographic inversion of the amplitudes reliable.

Changes in the seismic properties associated to the excavation damage were not noticed. The zone of smaller velocities a few centimetres wide, seen in the tomograms close to the tunnel, is most probably due to ray bending near the tunnel.

An initial hypothesis has been that the distribution of the seismic properties around the *TBM* tunnel would be approximately symmetric with respect to the vertical diameter of the tunnel. This assumption was disproved by the tomographic experiment in the Round 2 radial holes. The two crosshole sections placed in lower right part of the tomographic area differ strongly from the others.

Anisotropy of the P-wave velocity has been noticed and it is consistent with the elastic model used. The magnitude of the anisotropy is *2%* and the direction is vertical.

For the small scale in question, the positioning precision required is in the millimeter range. This is one order of magnitude less than the borehole diameter and, therefore, not so easy to achieve, especially for larger depths in the hole. The distance estimates particularly prone to error are the

ones between a source and a receiver placed at the bottom of two different holes, in which case, positioning errors in each hole may build up.

An effective way to determine the needed position corrections is to always run down-hole tests in parallel with crosshole tests. It is much easier to keep a precise source- receiver distance along the same hole. The "true" velocities determined in this way can be used, together with the crosshole data, to bring the positioning accuracy under the required limit.

The radial hole setup has been, so far, one of the more successful ways to detect and quantify changes in the rockmass due to excavation. Its possible drawback is that the experiment can not be run pre- and post-excavation. That may change if the boreholes are inclined with respect to the tunnel axis at an angle of appr. *45* , as shown in Figure 22. The length of the boreholes must be appr. *5 m*, for a radial fan similar to the present one.

By drilling the radial holes as in Figure 22, the measurements between these holes and the tunnel can be conducted for appr. *3.5 m* along the tunnel axis, and are likely to be more relevant than the downhole measurements done so far. Moreover, the measurements in the radial holes can be done before and after excavation, which will allow the direct measuring of possible changes.

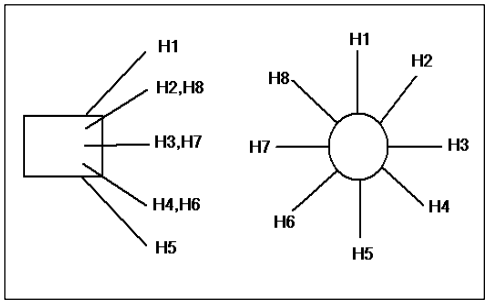


*Figure 22. Suggested layouts of radial boreholes, to allow experiments to be conducted before and after the excavation of the following tunnel section.*

## 7. Comments

The first objective of investigations could be met, in as much as both a near field disturbance with a thickness of up to *0.5 m* and a transition zone *1-5 m* to *2.5 m* deep were identified.

By determining the spatial variations of the seismic properties in the vicinity of the tunnel, the seismic part of the second and the third objective was also met. How the local stress changes reflect in the changed seismic properties and what are the outstanding features, if any, still remains to be determined.